Elasticity of a polydisperse hard-sphere crystal

Mingcheng Yang and Hongru Ma*
Institute of Theoretical Physics, Shanghai Jiao Tong University, Shanghai 200240, People's Republic of China
(Received 9 April 2008; revised manuscript received 3 June 2008; published 22 July 2008)

A general Monte Carlo simulation method of calculating the elastic constants of a polydisperse hard-sphere colloidal crystal is developed. Elastic constants of a size-polydisperse hard-sphere fcc crystal are calculated. The pressure and three elastic constants (C_{11}, C_{12}, and C_{44}) increase significantly with the polydispersity. It was also found from extrapolation that there is a mechanical terminal polydispersity above which a fcc crystal will be mechanically unstable.

DOI: 10.1103/PhysRevE.78.011404 PACS number(s): 82.70.Dd, 05.10.Ln, 62.20.−x

I. INTRODUCTION

Elastic constants are among the most important physical quantities describing macroscopic mechanical behaviors of a crystal. For hard-sphere crystals, the elastic constants have been calculated by various groups with different methods including density functional theory [1–5], Monte Carlo (MC) simulations [6–10], and molecular dynamics simulations [11,12] in the last two decades. The work of Jaric and Mohanty [1] and Jones [2] predicted a negative Poisson ratio in the hard-sphere crystal, which stimulated much interest in the investigation of the elasticity of this system. However, their predictions were proved incorrect by subsequent studies [3,4,6,11]. The hard-sphere system is the simplest of the systems which have a pure repulsion interaction; thus, the study of the elasticity of hard-sphere crystals is an excellent starting point to the studies of more complicated and realistic repulsive systems. Due to the simplicity of the hard-sphere system, it often serves as a simple model system for testing new theoretical approaches. The hard-sphere model is also an important model for a large class of colloid systems; understandings of colloid systems have greatly benefited from the extensive researches of the monodisperse hard-sphere model. A more realistic model describing hard-sphere colloidal systems is the size-polydisperse hard-sphere system. The size polydispersity of colloid particles is an intrinsic property of colloidal systems [13]. The polydispersity of colloidal hard spheres is characterized by the ratio of the standard deviation to the mean of the diameter. It has a remarkable influence on the thermodynamic and dynamic behaviors of the system [14–22]. It is natural to expect that the elastic constants of a polydisperse hard-sphere crystal differ from those of a monodisperse hard-sphere crystal. However, it seems that the problem of the elastic constants of polydisperse hard-sphere crystals is not properly addressed in the literature to the best of our knowledge.

In this work we propose a general Monte Carlo scheme to investigate the elasticity of a polydisperse hard-sphere system, by which we calculated the elastic constants of a size-polydisperse hard-sphere crystal. We only consider face-center-cubic (fcc) crystal structure in this study, as our previous calculations [23] showed that fcc structure is still the most stable one for a size-polydisperse hard-sphere crystal as in the monodisperse case. When simulating a polydisperse crystal the semigrand ensemble is the best candidate [15,24,25]. In the ensemble the imposed physical quantity is the chemical potential difference $\Delta\mu$ of particles of each kind to a reference kind. To obtain the chemical potential difference for a prescribed size distribution $\rho(\sigma)$, one has to solve a functional inverse problem [26–28], which can be accomplished easily by the semigrand ensemble version of the *nonequilibrium potential refinement* (NEPR) method (SNEPR method) [23].

Simulation approaches for calculating the elastic constants of a monodisperse hard-sphere crystal are divided into two categories. One is the "fluctuation" method [7] where elastic constants are related to the thermal averages of the corresponding stress components. There are some difficulties to extend the method to the polydisperse system. In the present paper we employ another method, the so-called "strain" method [6,8,10–12], where elastic constants can be obtained from the free-energy–strain relation or its first derivative, the stress-strain relation. In the simulation we used the extended ensemble method [23,29] to determine the Helmholtz free energy of the crystal with different strain, which can also be obtained by the thermodynamic integration method [30]. Then the elastic constants were extracted from the free-energy–strain data.

The paper is organized as follows. In Sec. II, we introduce the model and explain how the semigrand ensemble can be applied to calculate the elastic constants of polydisperse hard-sphere crystals. Section III describes the simulation method employed in this work. The computational details and results are provided in Sec. IV. Finally, we present our conclusions in Sec. V.

II. MODEL AND THEORY

A. Semigrand canonical emsemble

The semigrand canonical ensemble (SCE) is the most suitable ensemble for a simulation study of the elastic properties of a size-polydisperse hard-sphere crystal. In this ensemble the total number of particles and the distribution of particle sizes are fixed while the number of particles of each size is permitted to fluctuate. In the simulation study, the total number of particles in the system is usually limited to a

*hrma@sjtu.edu.cn

few hundreds to thousands, which is too small to distribute accurately according to a prescribed distribution of particle sizes. With the semigrand canonical ensemble, the distribution is realized through averages since the particle sizes are allowed to fluctuate. The grand canonical ensemble can also achieve the goal of distribution realization, but insertion and deletion of particles often require more computational resources. For a size-polydisperse system consisting of N particles with the composition distribution $\rho(\sigma)$ in a constant volume V, the Helmholtz free energy $F(N,V,\{\rho(\sigma)\},T)$ of the system is given by

$$F = -PV + N\int \mu(\sigma)\rho(\sigma)d\sigma, \tag{1}$$

where P is the pressure, σ is the diameter of the particles, and $\mu(\sigma)$ is the chemical potential of particles with diameter σ. The semigrand canonical free energy (SCFE) $Y(N,V,\{\mu(\sigma)\},T)$ is obtained from the Helmholtz free energy by the Legendre transformation

$$Y = F - N\int [\mu(\sigma) - \mu(\sigma_r)]\rho(\sigma)d\sigma, \tag{2}$$

where σ_r is the diameter of an arbitrarily chosen reference component. The SCFE $Y(N,V,\{\mu(\sigma)\},T)$ is a functional of $\mu(\sigma)-\mu(\sigma_r)$. In the semigrand canonical ensemble the thermodynamic variable to characterize the equilibrium system is $\mu(\sigma)-\mu(\sigma_r)$ rather than the composition distribution $\rho(\sigma)$.

The partition function γ for this ensemble is [31]

$$\gamma = \frac{1}{N!}\int_{\sigma_1}\cdots\int_{\sigma_N} Z_N\left[\prod_{i=1}^{N}\frac{1}{\Lambda^3(\sigma_i)}\right] \times\exp\left\{\beta\sum_{i=1}^{N}[\mu(\sigma_i)-\mu(\sigma_r)]\right\}\prod_{i=1}^{N}d\sigma_i; \tag{3}$$

here, $\Lambda(\sigma_i)=h/(2\pi m_i kT)^{1/2}$ is the thermal wavelength of the ith particle and Z_N is the canonical configuration integral for a given size configuration:

$$Z_N = \int_{r_1}\cdots\int_{r_N} e^{-\beta U}\prod_{i=1}^{N}d\mathbf{r}_i. \tag{4}$$

By introducing the excess chemical potential relative to the ideal gas $\mu_{ex}(\sigma_i)=\mu(\sigma_i)-kT\ln(\frac{N\Lambda(\sigma_i)^3}{V})$, we can rewrite γ in a more symmetric form

$$\gamma = \frac{1}{N!\Lambda^{3N}(\sigma_r)}\int_{\sigma_1}\cdots\int_{\sigma_N} Z_N \times\exp\left\{\beta\sum_{i=1}^{N}[\mu_{ex}(\sigma_i)-\mu_{ex}(\sigma_r)]\right\}\prod_{i=1}^{N}d\sigma_i. \tag{5}$$

The partition function γ is related to the thermodynamic potential Y through

$$Y = -kT\ln\gamma(N,V,T,\mu_{ex}(\sigma)-\mu_{ex}(\sigma_r)). \tag{6}$$

In practical simulations the diameter of particles are discretized into a series of special particle sizes or divide the total size range of particles into many small bins [27,28]. As a result, the semigrand canonical partition function γ becomes

$$\gamma = \frac{1}{N!\Lambda^{3N}(\sigma_r)}\sum_{\sigma_1=\sigma_{min}}^{\sigma_{max}}\cdots\sum_{\sigma_N=\sigma_{min}}^{\sigma_{max}} Z_N \times\exp\left\{\beta\sum_{i=1}^{N}[\mu_{ex}(\sigma_i)-\mu_{ex}(\sigma_r)]\right\}; \tag{7}$$

here, σ_{min} and σ_{max} are, respectively, the minimum and maximum of particle sizes.

B. Elastic constants of a size-polydisperse solid

The elasticity of a solid is the property that the solid deforms in response to an external stress and returns to its initial configuration when the stress is removed. Usually the deformation is small; otherwise, the deformation may become permanent. In the case of hard-sphere solids, the situation is more complicated because an external stress is necessary to stabilize the solid, while the deformation of the solid is induced by exerting an excess external stress. The deformation of a continuous solid can be described by the Lagrangian strain tensor

$$\eta_{ij} = \frac{1}{2}\left(\frac{\partial u_i}{\partial x_j} + \frac{\partial u_j}{\partial x_i} + \frac{\partial u_k}{\partial x_i}\frac{\partial u_k}{\partial x_j}\right); \tag{8}$$

here, u_i is the ith component of the displacement field and x_i is the ith component of the position of the displaced point in the solid; repeated indices are summed from 1 to 3. The Helmholtz free-energy density $f=F/V$ (where V is the volume of the undeformed solid) is a functional of the strain field. For a homogeneous deformation—namely, the Lagrangian strain tensor—η_{ij} is independent of the position and the free-energy density becomes a function of the constant strain. The elastic constants can be defined in terms of the following Taylor expansion of the free-energy density:

$$f(\eta_{ij}) = f(\mathbf{0}) + T_{ij}(\mathbf{0})\eta_{ij} + \frac{1}{2}C_{ijkl}\eta_{ij}\eta_{kl} + \cdots, \tag{9}$$

where $f(0)$ is the Helmholtz free-energy density of the unstrained solid and $T_{ij}(0)$ is the stress tensor of the unstrained solid which is necessary to stabilize the hard-sphere crystal, in the case of an fcc hard-sphere solid, $T_{ij}(0)=-p\delta_{ij}$, where p is the hydrostatic pressure. The C_{ijkl} are the second-order elastic constants.

It should be emphasized that in the case of a size-polydisperse system, the composition distribution of the strained system must remain the same as that of the unstrained system; this is because η_{ij} and $\rho(\sigma)$ are two independent variables of the Helmholtz free energy. Thus the explicit expression of elastic constants is

$$C_{ijkl} = \left.\frac{\partial^2 f(\eta)}{\partial\eta_{ij}\partial\eta_{kl}}\right|_{\rho(\sigma);\eta=0}. \tag{10}$$

Here the subscript $\rho(\sigma)$ means that the distribution of particle sizes is fixed during the application of strain. In the semi-

grand canonical ensemble, the Helmholtz free-energy density of the strained system with strain tensor η and composition distribution $\rho(\sigma)$ is

$$f(\eta) = y(\eta) + \frac{N}{V}\int [\mu(\sigma,\eta) - \mu(\sigma_r,\eta)]\rho(\sigma)d\sigma$$

$$= y(\eta) + \frac{N}{V}\int [\mu_{ex}(\sigma,\eta) - \mu_{ex}(\sigma_r,\eta)]\rho(\sigma)d\sigma$$

$$+ \frac{3NkT}{V}\int \ln\left(\frac{\Lambda(\sigma)}{\Lambda(\sigma_r)}\right)\rho(\sigma)d\sigma; \quad (11)$$

here, $y=Y/V$. In the semigrand ensemble the composition distribution $\rho(\sigma)$ depends not only on the chemical potential difference, but also on the strain η_{ij}. Therefore, in order to keep the composition distribution unchanged, the chemical potential difference $\mu_{ex}(\sigma,\eta)-\mu_{ex}(\sigma_r,\eta)$ has to be adjusted for each strain η_{ij}. That means at each given strain the chemical potential difference is recalculated. The evaluation of the chemical potential difference for a given composition distribution and strain can easily be performed by the SNEPR method [23], explained in the following subsection.

For the size-polydisperse hard-sphere fcc crystal, there are only three independent second-order elastic constants C_{1111}, C_{1122}, and C_{1212}. In Voigt notation they can be written in a more compact format: $C_{11}=C_{1111}$, $C_{12}=C_{1122}$, and $C_{44}=C_{1212}$. It should be noted that the elastic constants defined in this way is not the one that is measured directly in experiments, though it is widely used in theoretical investigations [5,6,9–12].

For a cubic crystal (including fcc structure) under isotropic pressure P the experimentally measured elastic constants C^T are related to the above-defined C by the following relations [4]:

$$C_{11}^T = C_{11} - P, \quad C_{12}^T = C_{12} + P, \quad C_{44}^T = C_{44} - P. \quad (12)$$

It is only when $P=0$ that the two sets of elastic constants coincide. A detail discussion of the elastic constants under stress can be found in [32].

III. SIMULATION METHOD

A. SNEPR method

In order to fix the composition distribution of the polydisperse crystal, we extend the NEPR algorithm [28] to the semigrand canonical ensemble. The algorithm can be used to find the chemical potential difference for a prescribed composition distribution—i.e., $\Delta\mu_{ex}(\sigma)=\Delta\mu_{ex}(\{\rho(\sigma)\})$—at a given strain. Here, we only give a brief description of the method. A detailed presentation can be found in Refs. [23,28]. For a given particle size distribution and strain, the chemical potential difference can be calculated by a Monte Carlo iteration procedure. First, an initial guess of the excess chemical potential is assigned to the implemention of a semigrand canonical ensemble simulation, and then it is modified at every few MC steps according to the instant size distribution $P_{ins}(\sigma)$ as follows:

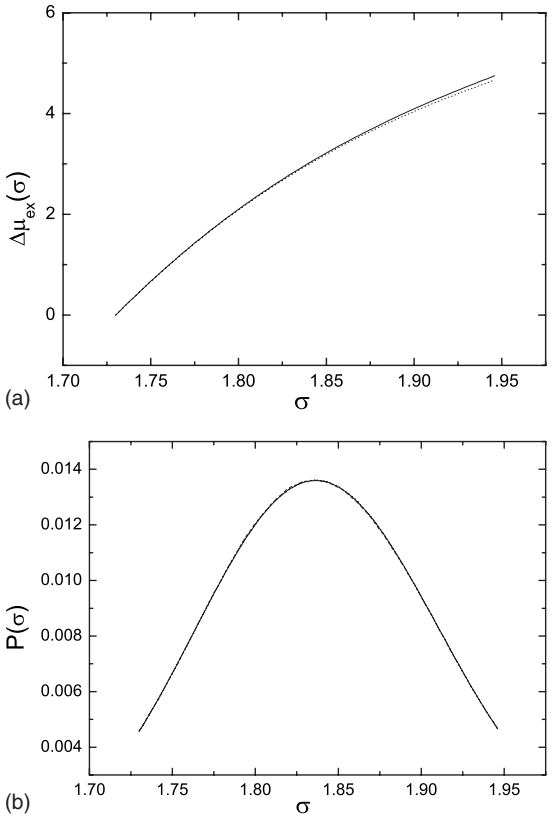

FIG. 1. (a) The solved excess chemical potential as function of the diameter of particles. The dotted line corresponds to the unstrained crystal and the solid line to the crystal with a contraction strain. (b) The solid line is the plot of the truncated Schultz function. The dotted and dashed lines are, respectively, the composition distribution for the unstrained and strained crystals, which are obtained from simulation by using the $\Delta\mu_{ex}(\sigma)$ plotted in (a). It is difficult to distinguish the three distributions.

$$\Delta\mu'_{ex}(\sigma) = \Delta\mu_{ex}(\sigma) - \gamma_i\left(\frac{P_{ins}(\sigma) - P(\sigma)}{P_{ins}(\sigma)}\right) \quad \forall \ \sigma. \quad (13)$$

Here γ_i is a modification factor of the ith iteration. When the difference of the average size distribution $\bar{P}(\sigma)$ and the given composition is less than a specified value ξ,

$$\xi \geqslant \max\left(\left|\frac{\bar{P}(\sigma) - P(\sigma)}{P(\sigma)}\right|\right), \quad (14)$$

one loop of the iteration is finished. The modification factor is then reduced, and the excess chemical potential of the last iteration is used as the initial input and starts the next iteration. The iteration continues until the modification factor γ reaches a very small value, typically 10^{-5}, and the resulting excess chemical potential is then regarded as the solution of the problem.

In order to check the validity of the SNEPR method, we apply it to both unstrained and strained polydisperse hard-sphere crystals. Figure 1(a) shows the calculated excess chemical potential for the truncated Schultz distribution as a function of the diameter of particles. The lower dotted and upper solid lines correspond to the unstrained crystal and the

crystal with a contraction strain 0.004, respectively. In the contracted crystal it is more difficult to increase the particle size, so a higher excess chemical potential is necessary to fix the composition distribution. Figure 1(b) shows the comparison of the given Schultz distribution and the distribution generated with the calculated excess chemical potential. In Fig. 1(b) we plot three lines of the distribution: the solid line is the given distribution, the dotted line is the distribution generated from the chemical potential difference for the unstrained crystal, and the dashed line is the one for the strained crystal. The agreement among the three distributions is excellent and nearly undistinguishable in the figure.

B. Free-energy difference calculation

To determine the elastic constants one only needs to know the Helmholtz free-energy difference between the unstrained and strained systems with the same composition distribution. The Helmholtz free-energy difference can be decomposed into two parts according to Eq. (11):

$$\Delta f(\eta) = \Delta y(\eta) + \Delta\left\{\frac{N}{V}\int [\mu_{ex}(\sigma,\eta) - \mu_{ex}(\sigma_r,\eta)]\rho(\sigma)d\sigma\right\}, \tag{15}$$

where Δ denotes the excess quantities relative to the unstrained system. Correspondingly, the elastic constants becomes

$$C_{ijkl} = \left.\frac{\partial^2[\Delta f(\eta)]}{\partial\eta_{ij}\partial\eta_{kl}}\right|_{\rho(\sigma);\eta=0}. \tag{16}$$

The second term on the right-hand side of (15) can be calculated when the $\mu_{ex}(\sigma_i,\eta)-\mu_{ex}(\sigma_r,\eta)$ for the fixed composition is determined. Our main task is thus to compute the difference of the semigrand free energy $\Delta y(\eta)$. To this end an extended ensemble [33] is introduced. The Lagrangian strain tensor η is regarded as an additional ensemble variable and a different η corresponds to a different macroscopic state. The partition function of the extended ensemble is defined as

$$\Gamma(N,T,\rho(\sigma)) = \sum_{\eta=0}^{\eta_{max}} \gamma(N,\eta,T,\mu_{ex}(\sigma,\eta) - \mu_{ex}(\sigma_r,\eta)), \tag{17}$$

where η_{max} denotes the state with maximum strain and all macroscopic states η possess the same composition distribution $\rho(\sigma)$. From Eqs. (6) and (17) the $\Delta y(\eta)$ becomes

$$\Delta y(\eta) = \ln\left[\frac{\gamma(N,0,T,\mu_{ex}(\sigma,0) - \mu_{ex}(\sigma_r,0))}{\gamma(N,\eta,T,\mu_{ex}(\sigma,\eta) - \mu_{ex}(\sigma_r,\eta))}\right] = \ln\left[\frac{\gamma(0)/\Gamma}{\gamma(\eta)/\Gamma}\right] = \ln\left[\frac{\Pr(0)}{\Pr(\eta)}\right], \tag{18}$$

where $\Pr(\eta)$ is the probability that the system is in the macroscopic state η. Therefore, knowledge of the macroscopic state probability distribution is sufficient to evaluate the elastic constants. The probability can be calculated from the simulation by flat histogram methods [34–36]. Here we demonstrate the implementation in the Wang-Landau scheme; other schemes can also be implemented.

The extended ensemble Monte Carlo simulation involves three kind of moves: the first is the particle displacement, the second is the particle resizing, and the third is the deformation of the simulation box which corresponding to the walk in the stain η space. The first two moves are accepted or rejected in the usual Metropolis way; i.e., if no overlap between particles happens, the trial move $(r,\sigma)\rightarrow(r',\sigma')$ is accepted with probability

$$P_{acc}(r,\sigma\rightarrow r',\sigma') = \min\{1,\exp[\beta\Delta\mu_{ex}(\sigma',\eta) - \beta\Delta\mu_{ex}(\sigma,\eta)]\} \tag{19}$$

where $\Delta\mu_{ex}(\sigma,\eta)=\mu_{ex}(\sigma,\eta)-\mu_{ex}(\sigma_r,\eta)$. The trial move in the η space is treated with the Wang-Landau sampling in order to obtain the macroscopic state probability distribution $\Pr(\eta)$. With a initial guess of $\Pr(\eta)$, the acceptance and rejection criteria for the simulation box deformation, $\eta\rightarrow\eta'$, are

$$P_{acc}(\eta\rightarrow\eta') = \begin{cases} \min\left\{1,\dfrac{\Pr(\eta)}{\Pr(\eta')}\left(\dfrac{V'}{V}\right)^N \exp\left\{\beta\sum_{\sigma}[\Delta\mu_{ex}(\sigma,\eta') - \Delta\mu_{ex}(\sigma,\eta)]\right\}\right\} & \text{if no overlap of spheres} \\ 0 & \text{otherwise} \end{cases} \tag{20}$$

where η only takes some discrete values $\eta_1,\eta_2,\ldots,\eta_n$. The chemical potential difference for each strain η was calculated with the SNEPR method and stored before the simulation with extended ensemble. During the extended ensemble simulation the (unnormalized) $\Pr(\eta)$ is updated by multiplying a modification factor $f>1$ when a state of η is visited; a histogram of the distribution in η of the visited states is recorded to monitor the convergence of $\Pr(\eta)$. The relative probability distribution of η is obtained at the end of the simulation, which is then used to determine $\Delta y(\eta)$ from Eq. (18). Because the composition distribution $\rho(\sigma)$ is prescribed in advance, substituting $\rho(\sigma)$, $\Delta\mu_{ex}(\sigma,\eta)$, and $\Delta y(\eta)$ into (15) the Helmholtz free-energy density difference $\Delta f(\eta)$ can then be determined. Finally, the elastic constants can be obtained from a polynomial fit to the free-energy–strain data.

IV. SIMULATION DETAILS AND RESULTS

Most of the simulations are performed with a system of 256 size-polydisperse hard spheres in a parallelepiped box; periodic boundary conditions are used in all three directions. The initial configuration is an ideal fcc crystal (zero strain). The density of the undeformed crystal taken in this simulation is $\rho=0.576$. This value is chosen because there are some known results of the terminal polydispersity [15] and the elastic constants in the monodisperse case [12] in the literature. As with the previous computations [6,9–11] the elastic constants of fcc crystals can be determined completely from three independent deformations. They are the contraction, contraction-expansion, and shear deformation. The composition distribution of particles used in the simulation is the truncated Schultz function

$$P(\sigma)=\frac{1}{z!}\left(\frac{z+1}{\bar{\sigma}}\right)^{z+1}\sigma^{z}\exp\left[-\left(\frac{z+1}{\bar{\sigma}}\right)\sigma\right] \quad \sigma_{min}\leqslant\sigma\leqslant\sigma_{max}, \tag{21}$$

where σ_{min} and σ_{max} are, respectively, the minimum and maximum diameters of hard-sphere particles. $\bar{\sigma}$ is the average diameter and $z=\delta^{-2}-1$ controls the width of the distribution. The criterion of the truncation is that the probability densities at both ends of the distribution are almost equal. They are several times less than the maximum probability density, as shown in Fig. 1(b). Here the probability density at σ_{min} and σ_{max} is 1/3 of the peak value. In the present paper the effect of the cutoff is not studied; the emphasis is on the effect of polydispersity to the elastic properties. The size-polydisperse degree is defined by $\delta=\frac{\sqrt{(\sigma-\bar{\sigma})^2}}{\bar{\sigma}}$. In the simulation we consider a uniform discrete set of diameters of particles. When the number of discrete diameters is large enough, the diameter of particles tends to a continuous variable which can resemble the real polydisperse system. In this study 101 different sizes of diameters were used.

As mentioned above, the composition depends not only on the chemical potential difference, but also on the strain tensor. Therefore, the chemical potential differences are calculated before the extended ensemble simulation is performed. The results indicate that the chemical potential difference increases with the magnitude of the strain, as plotted in Fig. 1(a). In the case of a contraction deformation, the increase of the chemical potential difference is more significant than the case of shear deformation. This is reasonable because the contraction deformation consumes more configuration space so that the turn to larger sizes is more difficult and requires a larger chemical potential.

We performed simulations for four different size polydispersity, simulation parameters, and results are given in Table I. The maximum polydispersity taken in our simulation is 5%, because at higher δ the crystal may be unstable [14,15,38]. In order to check the system size dependence we performed simulations for a larger system with particle number $N=2048$. The difference between the two systems is clearly less than or on the same order of the statistical errors, which indicates that a system of 256 particles is already large enough to get reasonable results, similar to the monodisperse hard-sphere system [10,12]. We also calculated the elastic constants of a monodisperse hard-sphere crystal using the present method, which are in full agreement with the results of Pronk and Frenkel [12]. From Table I we see that the pressure increases with increase of the size polydispersity and the pressure with $\delta=0.05$ is about 20% higher than the monodisperse system, which is consistent with previous reports [17,18] that the size polydispersity can induce a higher osmotic pressure in the hard-sphere colloidal crystal. A new phenomenon which has not been reported previously is that as the size polydispersity increases, all elastic constants (C_{11}, C_{12}, and C_{44}) of a fcc hard-sphere crystal increase significantly. At $\delta=0.05$, C_{12} is 1.3 times larger than that of the monodisperse system. Figure 2 shows the ratios of C_{11} to C_{12} and C_{44} to C_{12} as a function of the polydispersity δ. It is interesting to note that for the polydispersity used in the simulation these ratios nicely follow a linear relation with the polydispersity. Experimentally, Phan *et al.* have measured the high-frequency shear modulus for hard-sphere colloidal crystals [37]. Their results are comparable to the static shear moduli of the fcc crystal obtained in this study. Furthermore,

TABLE I. Elastic constants of fcc hard-sphere crystals and simulation parameters. All undeformed systems have the same density $\rho=0.576$. Here, δ is the size polydispersity, N the number of particles, and P the pressure of the hard-sphere crystal. The first two rows are the elastic constants of monodisperse hard-sphere crystals obtained from Ref. [12].

δ	N	P	C_{11}	C_{12}	C_{44}
0	256		115.5(10)	32.0(4)	72.4(3.2)
0	13292		117.4(4.4)	31.54(15)	71.96(11)
0	256	14.54(2.5)	115.1(46)	32.7(16)	72.0(35)
0.03	256	15.49(2)	125.1(47)	43.7(14)	77.1(45)
0.03	2048	15.528(6)	129.7(34)	47.3(12)	76.5(21)
0.039	256	16.24(2)	135.5(33)	55.9(10)	78.5(45)
0.05	256	17.34(1)	150.0(28)	73.6(8)	83.5(29)

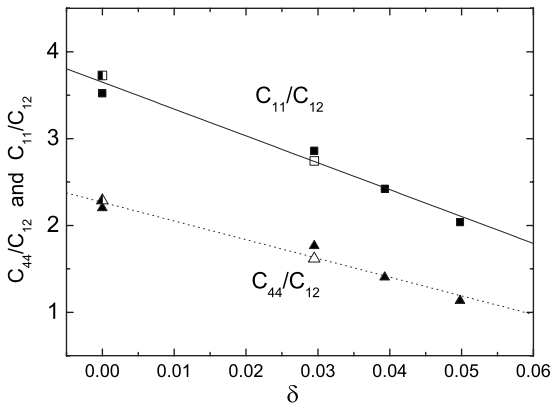

FIG. 2. The ratio of two elastic constants as a function of the size polydispersity δ. The triangles and squares indicate C_{11}/C_{12} and C_{44}/C_{12}, respectively. The solid symbols denote the data obtained from a 256-particle system, open symbols from a 2048-particle system. The semi-solid symbols are from a 13292-particle system given by Ref. [12]. The lines are linear fits to the data.

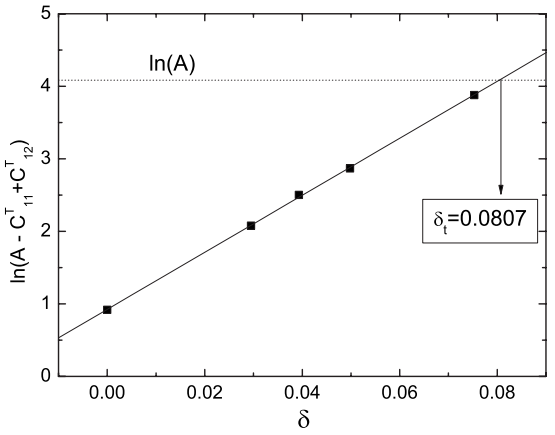

FIG. 3. The change of $C_{11}^T - C_{12}^T$ with the size polydispersity δ. The solid line is a linear fit to the data. The horizontal dotted line represents the function $y=\ln(A)$ and A is a fitted constant (see text). At $\delta=0.0807$ the solid line intersects with the dotted line.

our results indicate that the static shear modulus also increases with the polydispersity. We think that the effect can be detected experimentally from a precise measurement.

The monodisperse hard-sphere system was regarded as a representative model in the description of many different aspects of hard-sphere colloids. We expected that the polydispersity may give only a small correction to the monodisperse case. The large increase of the elastic constants with polydispersity indicates that the monodisperse model has its limitations in describing real hard-sphere colloids, especially in the elastic properties. The physics behind this large increase is still not clear; one general explanation is that the elastic constants are the second derivatives of the free energy, which should be more sensitive to the polydispersity than the free energy itself. A comprehensive understanding of this enhancement of elastic constants from polydispersity requires more extensive research which is beyond the scope of this paper.

As is well known, the necessary requirements for the stability of a cubic crystal (including fcc structure) are

$$C_{11}^T > 0, \quad C_{44}^T > 0, \quad C_{11}^T + 2C_{12}^T > 0, \quad (C_{11}^T)^2 - (C_{12}^T)^2 > 0. \tag{22}$$

For the polydisperse hard-sphere crystal under consideration, the first three conditions are obviously satisfied; the last one may be violated with increasing the polydispersity. Figure 3 depicts the change of $C_{11}^T - C_{12}^T$ with polydispersity. The value of $C_{11}^T - C_{12}^T$ decreases with increasing polydispersity and tends to zero at $\delta=0.0807$. To get this terminal polydispersity, we note that the simulation data follow a relation

$$C_{11}^T - C_{12}^T = A - e^{\alpha\delta+B},$$

which means that $\ln(A - C_{11}^T + C_{12}^T)$ depends linearly on the polydispersity δ, as shown in Fig. 3. Using the fitted value of $\ln A$ we can obtain the terminal polydispersity from extrapolation. This defines a mechanical terminal polydispersity (MTP) where the fcc crystal becomes unstable. The strain related to the coefficient $C_{11}^T - C_{12}^T$ is the following contraction-expansion deformation:

$$x' = (1+\epsilon)x, \quad y' = \frac{1}{1+\epsilon}y, \quad z' = z. \tag{23}$$

That is to say, for $\delta \geqslant 0.0807$ the fcc crystal is no longer stable under the deformation. The instability can also be described from the point of view of a soft mode. By solving the dispersion equation, one easily finds that there exists a transverse wave, which propagates along the diagonal of the (001) crystal plane, is polarized in the xy plane, and has the dispersion relation $\rho_m\omega^2 = \frac{1}{2}(C_{11}^T - C_{12}^T)k^2$ [39]; here, ρ_m is the mass density, ω is the circular frequency, and k the wave vector. Therefore, its frequency decreases substantially as the MTP is approached and this branch of the wave corresponds to a soft acoustical mode.

For the hard-sphere crystal, it is known that there is another terminal size polydispersity [14–16,38] above which the crystal will not be the most stable structure and a disorder solid phase [38] or solid-solid coexistence phase [16] may become the most stable equilibrium state. We refer to the terminal polydispersity as thermodynamical terminal polydispersity (TTP). The MTP has to be not lower than the TTP, since above TTP the fcc crystal exists in a metastable state and has good mechanical behaviors. Therefore, the MTP obtained in this study gives an upper limit of the TTP.

One important point of the semigrand canonical ensemble simulation of polydisperse hard-sphere crystal is the swapping of particles. In this ensemble the particle sizes are allowed to fluctuate to get the required size distribution; with the fluctuation, particles of different sizes effectively exchange their spatial positions constantly, and with a sufficiently long simulation, the equilibrium state is realized during the simulation. The calculated elastic constants in this simulation are the equilibrium elastic constants; we refer to them as ideal elastic constants. On the other hand, in real colloid crystals the particles cannot exchange their positions simply because the free-energy barrier is too high to be overcome in any reasonable time period. The particle arrangements are basically fixed by the process of crystal growth, which is not necessarily the equilibrium arrangement. It also noted that during the strain in the measurement of elastic constants the particles can only undergo small displacements, and it is not possible for particles to swap their positions. Based on this observation, a natural question is whether the simulated elastic constant is the same one in a measurement. The answer to this question is probably yes. The reason is that measurements are always performed with a crystal of macroscopic size, which contains much more colloid particles than the number of particles in the simulation study. If the sample is well relaxed, the self-averaging effect of the macroscopic number of particles may compensate the effect of particle nonswap. We expect that the ideal elastic constant can be experimentally measured after sufficient equilibration. To test the possible deviation from the ideal elastic constants, we also performed simulations in the canonical ensemble. We randomly picked up several configurations from the particle sizes distribution, and for each configuration the particle

TABLE II. Comparison of the pressure and elastic constants obtained from the semigrand canonical ensemble simulation (upper row) and the canonical ensemble simulation (lower row).

	P	C_{11}	C_{12}	C_{44}
Semigrand	15.528	129.7	47.3	76.5
Canonical	15.591	137.4	49.9	75.7

size was then fixed in the subsequent simulations of applying strains and extracting elastic constants. For a system of 2048 particles we find that elastic constants with different configuration realizations of the same distribution give elastic constants within 10% of difference. The average of the results from different realization of the configuration is listed in Table II.

V. CONCLUSION

To conclude, the elastic constants of a fcc polydisperse hard-sphere crystal are simulated by the Monte Carlo method with a semigrand ensemble; the composition distribution is fixed in the simulation by the SNEPR method. The results show that both the pressure of the hard-sphere solid and the three elastic constants increase with the size polydispersity δ. The method can be extended to the soft-sphere system and the system with other polydisperse attributes in a straightforward manner. Our results also indicate that there is a MTP where the fcc crystal is unstable, which provides us an upper limit of TTP. Above TTP we do not know which of the two structures (disorder solid and solid-solid coexistence phases) is the most stable one. Determining the stable state from computer simulations requires more effort to accomplish.

ACKNOWLEDGMENTS

The work was supported by the National Natural Science Foundation of China under Grant No. 10334020 and in part by the National Minister of Education Program for Changjiang Scholars and Innovative Research Team in University. We thank the anonymous referees for helpful suggestions.

[1] M. V. Jaric and U. Mohanty, Phys. Rev. Lett. **58**, 230 (1987); **59**, 1170 (1987).
[2] G. L. Jones, Mol. Phys. **61**, 455 (1987).
[3] E. Velasco and P. Tarazona, Phys. Rev. A **36**, 979 (1987).
[4] H. Xu and M. Baus, Phys. Rev. A **38**, 4348 (1988).
[5] B. B. Laird, J. Chem. Phys. **97**, 2699 (1992).
[6] K. J. Runge and G. V. Chester, Phys. Rev. A **36**, 4852 (1987).
[7] O. Farago and Y. Kantor, Phys. Rev. E **61**, 2478 (2000).
[8] S. Sengupta, P. Nielaba, M. Rao, and K. Binder, Phys. Rev. E **61**, 1072 (2000).
[9] S. K. Kwak and D. A. Kofke, Phys. Rev. B **70**, 214113 (2004).
[10] K. V. Tretiakova and K. W. Wojciechowskib, J. Chem. Phys. **123**, 074509 (2005).
[11] D. Frenkel and A. J. C. Ladd, Phys. Rev. Lett. **59**, 1169 (1987).
[12] S. Pronk and D. Frenkel, Phys. Rev. Lett. **90**, 255501 (2003).
[13] A. v. Blaaderen and A. Vrij, Langmuir **8**, 2921 (1992).
[14] P. N. Pusey and W. van Megen, Nature (London) **320**, 340 (1986).
[15] P. G. Bolhuis and D. A. Kofke, Phys. Rev. E **54**, 634 (1996); D. A. Kofke and P. G. Bolhuis, *ibid.* **59**, 618 (1999).
[16] M. Fasolo and P. Sollich, Phys. Rev. Lett. **91**, 068301 (2003).
[17] S. Phan, W. B. Russel, Z. Cheng, J. Zhu, P. M. Chaikin, J. H. Dunsmuir, and R. H. Ottewill, Phys. Rev. E **54**, 6633 (1996).
[18] S. Phan, W. B. Russel, J. Zhu, and P. M. Chaikin, J. Chem. Phys. **108**, 9789 (1998).
[19] S. Martin, G. Bryant, and W. van Megen, Phys. Rev. E **67**, 061405 (2003).
[20] R. P. A. Dullens and W. K. Kegel, Phys. Rev. Lett. **92**, 195702 (2004).
[21] V. Villeneuve, R. Dullens, D. Aarts, E. Groeneveld, J. Scherff, W. Kegel, and H. Lekkerkerker, Science **309**, 5738 (2005).
[22] H. J. Schope, G. Bryant, and W. van Megen, Phys. Rev. Lett. **96**, 175701 (2006).
[23] M. C. Yang and H. R. Ma, J. Chem. Phys. **128**, 134510 (2008).
[24] D. A. Kofke and E. D. Glandt, J. Chem. Phys. **87**, 4881 (1987).
[25] M. A. Bates and D. Frenkel, J. Chem. Phys. **109**, 6193 (1998).
[26] F. Escobedo, J. Chem. Phys. **115**, 5642 (2001); **115**, 5653 (2001).
[27] N. B. Wilding and P. Sollich, J. Chem. Phys. **116**, 7116 (2002).
[28] N. B. Wilding, J. Chem. Phys. **119**, 12163 (2003).
[29] M. C. Yang and H. R. Ma (unpublished).
[30] D. Frenkel and B. Smit, *Understanding Molecular Simulation* (Academic, San Diego, 1996).
[31] J. G. Briano and E. D. Glandt, J. Chem. Phys. **80**, 3336 (1984).
[32] T. H. K. Barron and M. L. Klein, Proc. Phys. Soc. London **85**, 523 (1965).
[33] A. P. Lyubartsev, A. A. Martsinovski, S. V. Shevkunov, and P. N. Vorontsov-Velyaminov, J. Chem. Phys. **96**, 1776 (1992).
[34] B. A. Berg and T. Neuhaus, Phys. Rev. Lett. **68**, 9 (1992).
[35] F. Wang and D. P. Landau, Phys. Rev. Lett. **86**, 2050 (2001); Phys. Rev. E **64**, 056101 (2001).
[36] J. S. Wang and R. H. Swendsen, J. Stat. Phys. **106**, 245 (2002).
[37] S. Phan, M. Li, W. Russel, J. Zhu, P. Chaikin, and C. T. Lant, Phys. Rev. E **60**, 1988 (1999).
[38] P. Chaudhuri, S. Karmakar, C. Dasgupta, H. R. Krishnamurthy, and A. K. Sood, Phys. Rev. Lett. **95**, 248301 (2005).
[39] L. D. Landau and E. M. Lifshitz, *Theory of Elasticity* (Beijing World Publishing, Beijing, 1999).